

Reflection of sound by concave surfaces

Martijn L.S. Vercammen

Peutz bv, Lindenlaan 41, PO Box 66, 6585 ZH, Mook, The Netherlands, m.vercammen@mook.peutz.nl

PACS: NO. 43.55.BR, 43.55.KA

ABSTRACT

Many spaces have curved walls or ceilings. With improved building technology and new fashions in architecture (blobs) there is an increasing number of problems due to the acoustic reflections by these surfaces. Sound reflected by concave surfaces will concentrate in a narrow area. In practical applications of room acoustics these curved surfaces will be calculated with a geometrical approach, mirror imaging, ray tracing or beam tracing. In computer programs the structure is modeled by flat segments. These geometrical methods do not correspond to reality. The only valid calculation method is the calculation from a wave extrapolation method. It is shown that a theoretical correct solution of the sound field by curved surfaces is possible. A fairly simple expression for the sound pressure in the focal point is found and a more complicated description of the reflected sound field by small curved surfaces is presented. Some formulas are presented to estimate the sound pressure due to focussing effects. Two cases are presented.

1. INTRODUCTION

Many small or large rooms have concave surfaces. With improved building technology and fashions in architecture (blobs) problems due to these surfaces are encountered more and more. Not only in the modern architecture but also in the old architecture these problems can occur. The influence of vaults is long known, see Figure 1.

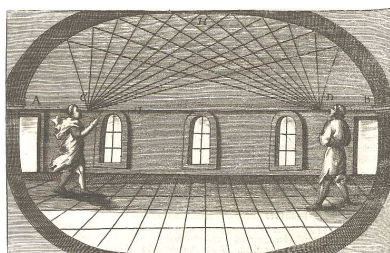


Figure 1. Illustration of the focussing effect by an ellipse [1]

Some situations are described in literature and many authors point out the danger of concave surfaces. In our consultancy

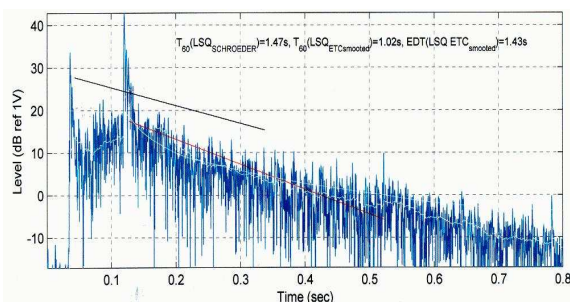


Figure 2. Example of an impuls response in a dome shaped hall (Tonhalle Düsseldorf before renovation)

work we had to deal with these situations e.g. in concert halls ([2],[3]). When sound is reflected from a concave surface the geometry of the surface will force the energy to concentrate. Figure 2 shows the impuls response (energy-time-curve ETC) of the Tonhalle Düsseldorf, before renovation. We see that a very significant echo occurs. Depending on the level and the time delay the sound concentration may cause an echo, sound colouration or imbalance in an orchestra sound.

Despite of the attention that is paid to the phenomenon none of the many books on acoustics describes the amplitude of the sound field in the focus. In practical consultancy work often ray tracing algorithms are used to quantify the focussing. In this paper we will show the limitation of geometrical solutions and we describe a wave based method to solve the problem. This paper will concentrate on reflections from a spherically-curved surface, e.g. a hemisphere or a sphere segment. For comparison, results from literature of reflections from cylindrically-shaped surfaces will also be shown. Part of this work is also published in [4],[5].

2. GEOMETRICAL METHODS

Thin lens method

Figure 3 shows the geometrical situation with a hard, fully reflecting, concave surface characterised by the radius R , a source position S at distance s and a resulting focal point M at distance u . From this geometry the thin lens formula can be derived:

$$\frac{1}{u} + \frac{1}{s} = \frac{1}{f \cos \theta} \text{ with } R = 2f \quad (1)$$

The pressure of the sound field incident at Q on the reflector can be described by:

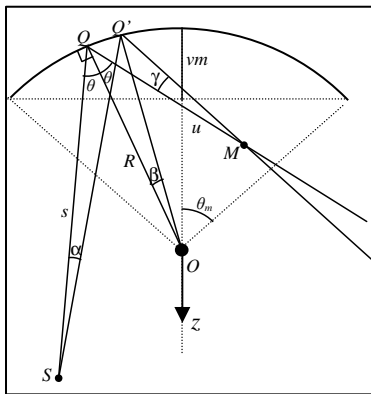


Figure 3. Geometry showing the concave surface with source position S and position of the focal point M

$$p(s) = \hat{p} \frac{e^{-iks}}{s} \quad (2)$$

where k =wavenumber and \hat{p} =amplitude (in [N/m]) corresponding to the value of the pressure amplitude at 1 m from the source

The geometrically-reflected sound field can be described using the position of the focal point as a reference. The pressure will depend on the distance r_M to the focal point, presuming r_M is in the illuminated area:

$$p(r_M) = X \frac{e^{-ik(s+u+r_M)}}{r_M} \quad (3)$$

At the surface of the reflector the pressure of (2) and (3) will be equal, resulting in:

$$p(r_M) = \hat{p} \frac{m}{s} \frac{e^{-ik(s+u+r_M)}}{|r_M|} = \hat{p} \frac{R \cos \theta}{2s - R \cos \theta} \frac{e^{-ik(s+d)}}{|d-u|} \quad (4)$$

where $d = u + r_M$. At $d = u$ (the mirror source M) the calculated sound pressure according to (4) will be *infinite*. In reality it will be finite and the pressure will depend on the wavelength and the size of the mirror. Outside this focal point the amplitude does not depend on the size of the mirror; the reception point is either visible or not. The sound pressure level increase ΔL_c compared to a flat reflector will be (see also [6],[7]):

$$\Delta L_c = -20 \log \left(\frac{1}{\left(\frac{1}{d} + \frac{1}{s}\right) R \cos \theta} - 1 \right) \quad (5)$$

This is for a double curved surface, with radius of curvature R in both directions. For cylindrical structures (curvature in one direction) $10 \log$ instead of $20 \log$ should be taken. The reduction by convex structures can be calculated using negative R .

Geometrical computer models

Computer models are used as a prediction tool for practical room acoustical purposes. The common prediction models are based on geometrical acoustics. Methods used are Image Source Method (ISM), Ray Tracing (RT) and Beam Tracing (BT). In this paragraph we discuss the applicability of these geometrical methods for the calculation of reflections from concave surfaces.

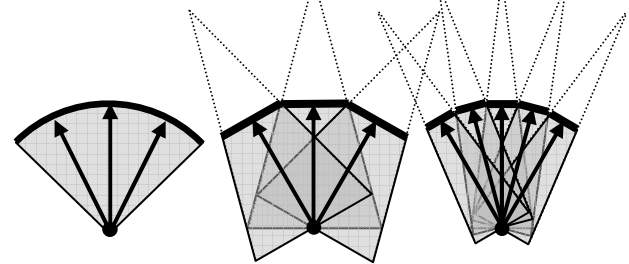


Figure 4. Illustration of the geometrical reflection by a continuous curvature (left) and segmented curvatures (middle and right)

In the practice of room acoustic modeling curved (sphere) elements are not modeled as curved elements but are replaced by small plane surfaces, segmenting the curved element (see figure 4). Depending on the shape of the curved segment, they are modeled as rectangle, trapezium or triangle planes. This segmenting will influence the calculated pressure in the focal point. The influence of segmenting also depend on the method used.

Image Source Method

The sound pressure in the center of a hemisphere using ISM can will be calculated and compared to the theoretical sound pressure discussed in chapter 3. Assuming the plane surfaces have characteristic dimension b , the area of each element will be b^2 . Applying ISM, for a hemisphere the number of mirror images will be:

$$N = 2\pi R^2 / b^2. \quad (6)$$

In ISM the energy of the visible image sources is added. In that case the pressure at distance r from a (mirror) source can be written by: $p(r)_{rms}^2 = \frac{1}{2} \hat{p}^2 / r^2$. With the source in the center of an hemisphere, the pressure in the center caused by the all the mirror sources at distance $r=2R$ will be:

$$p(0)_{rms}^2 = \frac{1}{2} N \hat{p}^2 / (2R)^2 \quad (7)$$

In chapter 3 it will be derived that the expected value for a hemisphere is: $p(0)_{rms}^2 = \frac{1}{2} \hat{p}^2 k^2$. This value can be obtained when the right number of plane surfaces is applied, so :

$$N = 4R^2 k^2 = (4\pi R / \lambda)^2 \quad (8)$$

That means that the number of surfaces required will be frequency dependant. For real situations in room acoustics, for example frequency 500 Hz and $R=10$ m, $N > 34000$. This is not practically feasible. The large number is due to the incorrect summation of energy of correlated sources.

If coherent sources will be used, including the phase in the summation of pressure, the number of surfaces can be reduced. Assuming a point source in the center of the sphere: $p(r) = \hat{p} e^{-ikr} / r$, the contribution of each image source in the center will be $p(r) = \hat{p} e^{-ik2R} / 2R$. When adding all image sources (with same phase) the total pressure in the center will be:

$$|p(0)| = N \hat{p} / 2R. \quad (9)$$

In chapter 3 it will be derived that the pressure in the focal point of a hemisphere is: $|p(0)| = \hat{p}k$. That means that a correct prediction in the focal point is obtained in case:

$$N = 2kR = 4\pi R / \lambda. \quad (10)$$

Again the number of surfaces required will be frequency dependant. For the calculation example given above $N=370$ is needed, this is much less as with energy summation and might even be practically possible.

The required width of the surfaces in this case will be:

$$b = \sqrt{2\pi R^2 / N} = \sqrt{\frac{1}{2}\lambda R} \quad (11)$$

in this example 1,3 m. This agrees with the required width of plane segments to model a cylinder as found by [8]. The illuminated width in the center by the mirror sources will be $2b$, in this case 2,6 m. In chapter 3 it is shown that in case of a hemisphere the actual width at the focal point is in the order of $\lambda/2$, so when $R > 2\lambda$, which is usually the case (except for small rooms at low frequencies), the focal area calculated with mirror images is too large. So by segmenting the curved surface and applying ISM it is not possible to predict both focal strength and width of the focal area correctly.

Ray Tracing

Ray tracing is used in many fields such as optics, seismic and acoustics. The propagating wave is modeled with a ray, normal to the propagating direction. The source is emitting the rays. Mostly, but not necessarily, with a uniform distribution. The sound power P of a monopole at distance d will be:

$$P = I \cdot S = \frac{\hat{p}^2}{2\rho c \cdot d^2} \cdot 4\pi d^2 = \frac{2\pi}{\rho c} \hat{p}^2 \quad (12)$$

Assuming the uniform distribution of N rays emitted by the source, the power P_i of each ray i will be:

$$P_i = \frac{2\pi}{\rho c} \frac{\hat{p}^2}{N} \quad (13)$$

The rays are detected with a receiver volume. The energy in that receiver volume depends on the travel time of the ray through the volume: $E_i = P_i \cdot \Delta t$, with $\Delta t = l_i / c$ and l_i = path length of ray i through the receiver volume. With the average intensity (averaged over the volume of the receiver) of the sound wave of ray i inside the receiver: $I_i = E_i \cdot c / V$, where V = volume of the receiver. This will result in:

$$I_i = \frac{P_i \cdot \Delta t \cdot c}{V} = \frac{P_i \cdot l_i}{V} \quad (14)$$

In case the model is segmented there will be a spread of energy around the focal point (see also figure 4). In case this spread is limited to $\lambda/2$ width, the dimensions of the segments should not be more than $\lambda/4$. Contrary to ISM, the pressure in the focal point will not increase when the number of segments further increases, since the number of rays that hit the focal area depends on the number of rays emitted from the source and the total opening angle of concave surface.

Next step is to consider an exact geometrical model in the sense that all rays reflect in the correct specular direction, depending on the orientation of the small surface element at impact position of the ray. This model can either be a parameterized model or a sufficiently segmented model.

Assuming all reflected rays will pass the exact focal point, the path length l through the receiver volume will be equal to the diameter of the receiver volume. The pressure of the reflection from a full sphere in the receiver volume results from energy summation:

$$p_{rms}^2 = \rho c \sum_{i=1}^N I_i = 12 \frac{\hat{p}^2}{D^2} \quad (15)$$

This sound pressure is independent on the number of rays but is dependant on the volume of the receiver. A larger receiver volume will not be compensated by more rays (as it will be in a statistical sound field) since all rays pass at the center. In chapter 3 it will be illustrated that in fact the energy will distribute over an area depending on the wavelength. When we assume the diameter of the receiver volume $D = \lambda/2$, the total pressure in the receiver volume will be:

$$p_{rms}^2 = 48 \frac{\hat{p}^2}{\lambda^2} \quad (16)$$

Which differs from the exact solution (chapter 3). For a half sphere the correspondence is deviation is larger. As with ISM, the basic problem is that an energy summation is used, where a amplitude summation would be required. Furthermore it is noted that in commercially available ray tracing programs the size of the receiver can not be chosen.

Beam Tracing

The main difference between RT and BT is the way how the decrease with distance is handled. In RT the decrease of sound pressure of an expanding sound field with the distance from the source is implicitly in the calculation method since the distance between the rays becomes larger and in a statistical approach the probability of hitting a (fixed size) volume receiver decreases. In BT the decrease with distance is calculated from:

$$p_{rms}^2 \cong \frac{\Delta\Omega}{S(r)} \quad (17)$$

where $\Delta\Omega$ is the opening angle of the beam and $S(r)$ is the cross-sectional area of the beam at distance r from the source. When applying this method on curved surfaces the beam will converge and due to the smaller $S(r)$ the geometrical correct increase of sound pressure will be found. In the focal point however $S(r) = 0$ which will lead to an (incorrect) infinite sound pressure. So this method is not capable of calculating the sound pressure in the focal point. Outside the focal point however this method can be applied and is expected to give basically the same results as ray tracing. As with RT, BT is used as an energy method, also called incoherent since phase is not included. Contrary to RT, BT is deterministic in the sense that at each position the pressure and phase can be calculated and the distance traveled, so a coherent calculation is basically possible. Outside the focal point coherent BT is capable of determining the interference pattern (see e.g.[9]).

It can be concluded that none of the methods give satisfactory results in the focal point. Better tools are needed to approximate the sound pressure field, especially around the focal point. Outside the focal point geometrical methods are sufficiently accurate to predict the average sound field. Interference might be incorporated by using coherent beam tracing.

3. WAVE BASED METHOD

Kirchhoff integral

Wave extrapolation uses the Huygens principle, developed by Christiaan Huygens in 1678 and later improved by Fresnel and Kirchhoff. According to the Huygens principle every point on the primary wavefront can be thought of as an emitter of secondary wavelets. The secondary wavelets combine to produce a new wavefront in the direction of propagation.

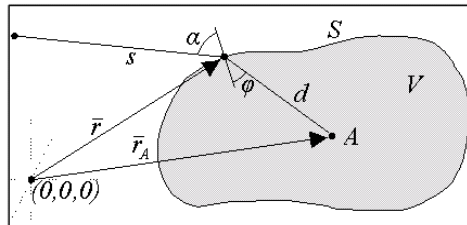


Figure 5. Geometry and notation used

The Kirchhoff integral states that for a point A in volume V with surface S the pressure can be calculated from the pressure at the surface and a dipole radiation from that surface element dS, with its axes normal to the surface (left part) and from the normal velocity at the surface S and a monopole distribution: (18)

$$p(r_A, \omega) = \frac{1}{4\pi} \int_S \left(p(r, \omega) \frac{1+jkd}{d} \cos \varphi \frac{e^{-jkd}}{d} + j\omega \rho \cdot v_n(r, \omega) \frac{e^{-jkd}}{d} \right) dS$$

As for the incident pressure on the surface S a monopole is assumed that generates a spherical sound field with pressure p at distance s, see (2), omitting the time dependence. The velocity at this point on S can be calculated from:

$$v(r, \omega) = -\frac{1}{i\rho\omega} \frac{\partial p}{\partial s} = \frac{1}{\rho c} \frac{1+jks}{jks} \hat{p} \frac{e^{-jks}}{s} \quad (19)$$

this results in a sound pressure in A:

$$p_A = \frac{\hat{p}}{4\pi} \int_S \left(\frac{1+jks}{s} \cos \alpha + \frac{1+jkd}{d} \cos \varphi \right) \frac{e^{-jk(s+d)}}{sd} dS \quad (20)$$

Spherical surfaces

Using polar co-ordinates with the origin in the center of the sphere, described by $x = R \sin \theta \cos \varphi$, $y = R \sin \theta \sin \varphi$, $z = R \cos \theta$, a small surface element can be described by $dS = R^2 \sin \theta d\theta d\varphi$ and the integral formulation for the pressure of a reflection from this surface becomes: (21)

$$p_A = \frac{\hat{p}R^2}{4\pi} \int_{\theta=0}^{\theta_m} \int_{\varphi=0}^{2\pi} \sin \theta \left(\frac{1+jkr}{r} \cos \varphi + \frac{1+jks}{s} \cos \alpha \right) \frac{e^{-jk(r+s)}}{rs} d\theta d\varphi$$

while integrating over the opening angle of the sphere segment θ_m . Some numerical results are shown in figure 6.

Pressure in the center of a sphere

For the specific situation of a full sphere, the source in the center and the receiver in the center, this formula simplifies to ($s=d=R$, $\cos \alpha = \cos \varphi = 1$):

$$p(0) = \frac{jk\hat{p}}{2\pi R^2} \left(1 + \frac{1}{jkR} \right) e^{-j2Rk} \int_S dS = j2k\hat{p} \left(1 + \frac{1}{jkR} \right) e^{-j2Rk} \quad (22)$$

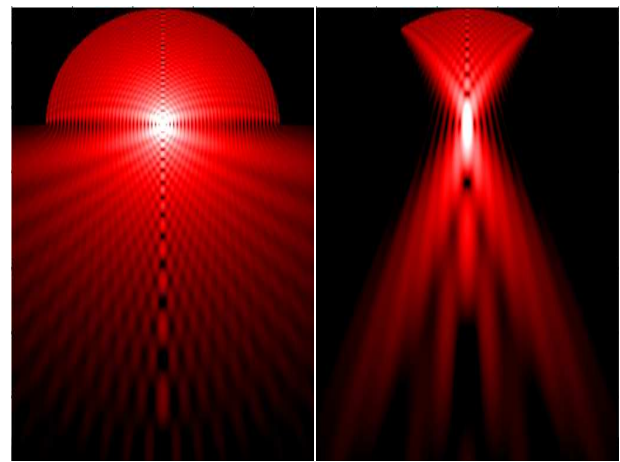


Figure 6. Numeric calculations of the reflected sound field based on (21). The radius R of the sphere segment is 5.4 m, $k=18.4$ ($kR=100$). The source is in the centre point. The difference between white and black is 30 dB. Left: $\theta_m = \pi/2$, Right: $\theta_m = \pi/5$

$$\text{for } kR \gg 1: p(0) = j2k\hat{p} \cdot e^{-j2kR} \quad (23)$$

or generalised for sphere segments with opening angle θ_m :

$$p(0) = jk\hat{p}(1 - \cos \theta_m) \cdot e^{-j2kR} \quad (24)$$

or in terms of rms pressure: $p_{rms}^2 = \frac{1}{2} \hat{p}^2 k^2 (1 - \cos \theta_m)^2$. The sound pressure level (SPL) at the focal point, relative to the SPL at 1m from the source, is:

$$\Delta L = 10 \log k^2 (1 - \cos \theta_m)^2 \quad (25)$$

For a hemisphere with $\theta_m = \frac{1}{2} \pi$: $\Delta L = 10 \log k^2$

It is noted that the increase in sound pressure level only depends on the opening angle and frequency and not on the radius of the (hemi)sphere (in case $kR \gg 1$). All energy radiated in the (hemi)sphere returns to the centre, independently from the radius.

Reflected sound field in a full sphere

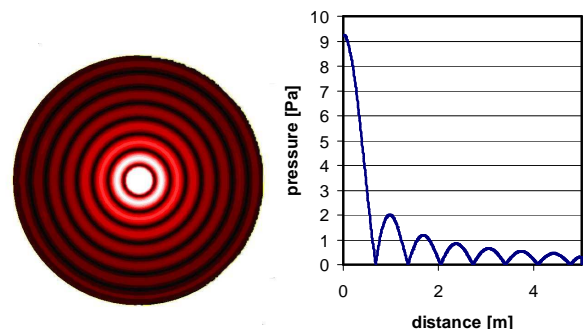


Figure 7. Reflected sound field in a full sphere. Numeric calculations with (21). $k=4.6$ (250 Hz), $R=5.4$ m

With the source in the center of a full sphere the sound pressure can be calculated with the spherical Bessel function j_0 :

$$p(r) = p(0) \cdot j_0(kr) = p(0) \cdot \frac{\sin kr}{kr} \quad (26)$$

The reflected sound field shows a strongly interfering standing wave pattern. Outside the focus point, the envelope of the

interference pattern correspondonds to the inverse square law ($p^2 \sim 1/r^2$).

Reflected sound field in the axis of a sphere segment

When using approximate solutions for (21), see [4], the pressure in the axis of a sphere segment (such as shown in Fig.6) can be calculated. With z being the coordinate along the axis (see Fig.3):

$$|p(z)| \approx \frac{2\hat{p}}{z} \sin\left(\frac{1}{2}kR(1-\cos\theta_m)\left|\frac{z}{R-z}\right|\right) \quad (27)$$

The sound field strongly depends on the ‘depth’ of the sphere segment $vm (=R(1-\cos\theta_m))$, see Fig.3), for which there are three situations:

I. $vm > \lambda$, or $kR(1-\cos\theta_m) > 2\pi$: The area around the focal point the pressure can be described by (27). For larger distance the average pressure can be estimated with a geometrical method (e.g.(4)), see fig.8. The two transition points are defined by:

$$z \approx \pm \frac{R\lambda}{R(1-\cos\theta_m) \pm \lambda} \quad (28)$$

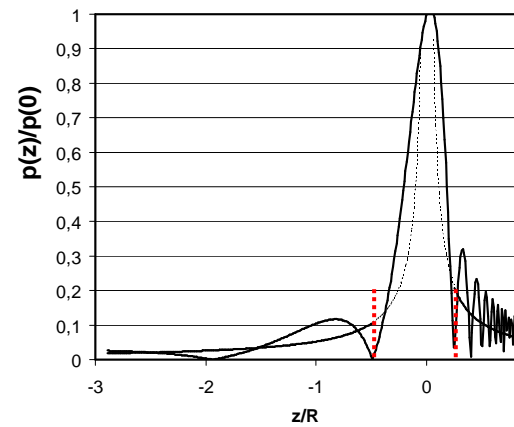


Figure 8. Reflected sound field along the axis of a sphere segment. Shown is the solution with (27) and the geometrical decrease. Transition points (in red) with (28). $kR(1-\cos\theta_m)=19$, see Fig. 6, right

II. $vm < \lambda/4$, or $kR(1-\cos\theta_m) < \pi/2$: When the depth of the segment is less than a quarter wavelength, diffraction from the

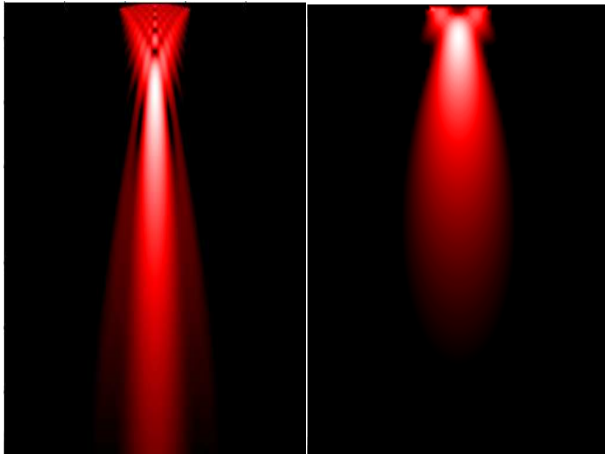


Figure 9. Numeric calculations of the reflected sound field based on (21). The source is in the centre of the sphere segment $\theta_m = \pi/10$, $R=5,4$ m. Left: $k=18,4$, $kR(1-\cos\theta_m)=4,8$, Right: $k=4,6$; $kR(1-\cos\theta_m)=1,2$

segment will occur, similar to, or even almost equal to, the low frequency diffraction from a flat disk (fig 9, right). The pressure amplitude will be inversely proportional to the distance from the sphere ($R-z$) instead of the distance from the centre of the sphere z :

$$|p(z)| = \hat{p} \frac{kR(1-\cos\theta_m)}{R-z} \quad (29)$$

In this situation no focussing effects due to the concave shape are to be expected.

III. $\lambda/4 < vm < \lambda$, or $\pi/2 < (kR(1-\cos\theta_m)) < 2\pi$: When the depth vm is between a quarter and a full wavelength a sort of beam will be obtained, as can be seen in fig.9, left. The high pressure at the focal point will spread over a certain distance.

Reflected sound field in the focal plane of a sphere segment

Again using approximate solutions for (21), see [4] and [5], the main lobe of the pressure in the focal plane of a sphere segment (perpendicular to the axis) can be calculated, with x is the distance to the focal point M in the focal plane:

$$|p(x)| \approx \hat{p}k(1-\cos\theta_m)\cos\left(\frac{1}{2}xk\sin\theta_m\right) \quad (30)$$

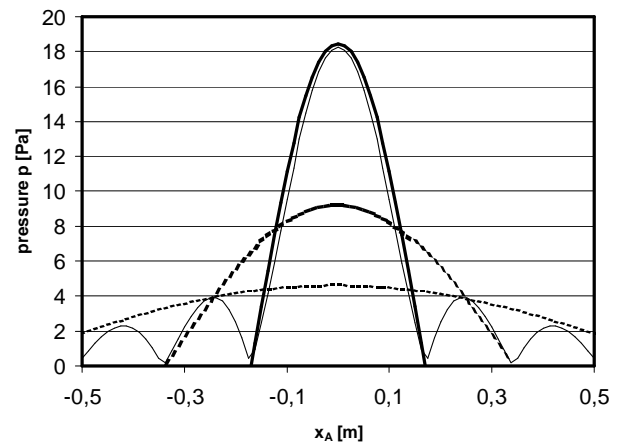


Figure 10. Reflected sound pressure in the focal plane of a sphere segment. $\theta_m = \pi/2$. Results for $k=18,4$ (1000 Hz), $k=9,6$ (500 Hz) and $k=4,8$ (250 Hz). Note that at $x=0$: $p(0)=k$ (with $\hat{p}=1$). For $k=18,4$: thin line is calculated with (21), solid line is approximation of main lobe with (30)

Figure 10 shows that for high frequencies the peak pressure in the focal point is higher, for lower frequencies the spread of the focal area is larger. The width of the focussing area (-3 dB points) can be approximated by: $x = \pm \lambda / (4 \sin\theta_m)$. At the focal (x,y) plane ($z=0$) of a hemisphere ($\theta_m = \pi/2$) the area where focussing will occur will be a circle with a diameter of half a wavelength: $S_M \approx \pi \left(\frac{\lambda}{4 \sin\theta_m} \right)^2 = \frac{\pi}{16} \lambda^2$ (31)

An alternative way to obtain an estimation of the pressure in the focal area would be to use an energy approximation, equally distributing the energy over this area. The sound power P_s of a sound source can be written: $P_s = 2\pi\hat{p}^2 / \rho c$. The power from a sound source in the centre, incident on a hemisphere, will be half this value: $P_l = \pi\hat{p}^2 / \rho c$. This sound power will be reflected towards the focal point. When distributing this sound power over the focussing area S_M the rms pressure will be:

$$p_{rms}^2 = \frac{\rho c P_I}{S_M} \approx 0,4 \hat{p}^2 k^2 \quad (32)$$

this is close to the theoretical peak value $p_{rms}^2 = \frac{1}{2} \hat{p}^2 k^2$ (24). So for a hemisphere, the energy is distributed over a circular area with a width of approximately half a wavelength.

Validation experiment

To verify the theoretical amplification in the focal point an experimental setup at small scale was made. It consists of an half ellipsoid with the two focal points at relatively small distance. The model is CAD/CAM milled from a solid polyurethane block (Ebaboard PW 920), a material with a high density and excellent low surface porosity. The accuracy of the shape of the ellipsoid is approx. 0.01 mm. The impulse response was measured with a MLS (Maximum Length Sequence) signal. In time domain the separation of direct signal and (single) reflected signal was made. The setup and frequency dependant difference between reflected and direct sound pressure level are shown in figure 11. The results show a very good agreement with the theory.

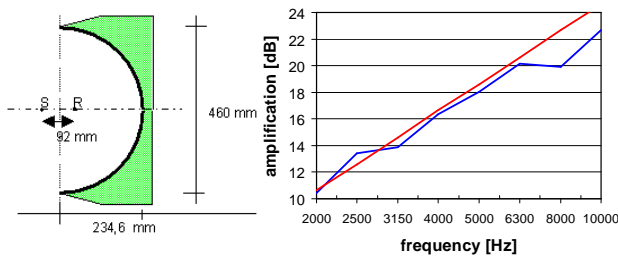


Figure 11. Left: Section of the experimental setup (half ellipsoid), S=source, R=microphone. Right: difference between SPL reflected and direct sound, red: theoretical (20) and blue: measured

4. PRACTICAL CONSIDERATIONS

Spheres, cylinders and ellipsoids

Many curved surfaces have a radius in one direction, e.g. the rear wall of many theatres. For cylindrical shapes there is concentration in one direction and divergence in the other direction. The SPL increase (re 1 m from the source) at the focal line of a cylindrical cylinder will be (see [8],[10]):

$$\Delta L = 10 \log \left(\frac{\pi k}{4R} \right) \quad (33)$$

Contrary to the sphere, the focussing effect in cylinders is depending on the radius R. Figure 12 shows the SPL increase

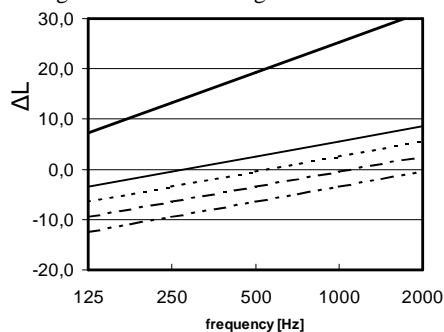


Figure 12. The ΔL (SPL in focus point relative to the SPL at 1 m from the source) at the focal point or focal line for: upper line: a hemisphere (25); lower lines: a half cylinder with radius (top-down): R=4, 8, 16 and 32 m (33). The SPL of the hemisphere is independent of the radius

at the focal point for some different conditions. It shows that the focussing effect of a spherical reflector is much stronger than the focussing effect of a cylinder. When comparing the level of the reflection relative to the direct sound at the receiver position, the level decrease of the direct sound has to be added. The amplification at the focal point can be quite dramatic, especially for spherically-curved structures.

More curved shapes are possible such as ellipsoids and elliptic cylinders. A number of cylindrical shapes is described in [10]. As for ellipsoid shapes the sound source can be in one focal point and the receiver in the other (as in the validation experiment). In those cases the amplification in the center is slightly reduced. Numerical experiments have shown that the pressure in the focal point of an ellipsoid can be approximated by (a and c being the small and long axis of a prolate ellipsoid):

$$|p| \approx 2 \hat{p} k (a/c)^{1,4} \quad (34)$$

In case the source is not in the center the focal point, axis and focal plane must be constructed based on geometrical rules. The pressure in the focal will however be lower (see [4]).

Reduction possibilities

Apart from changing the basic shape of the space (mostly the best option) the strength of the reflection in the focal point can be reduced by reducing the specular reflected energy. Incorporating the reflection factor R_s in (25):

$$\Delta L = 10 \log |R_s|^2 k^2 (1 - \cos \theta_m)^2 \quad (35)$$

with $\alpha = 1 - |R^2|$ this will result in:

$$\Delta L = 10 \log (1 - \alpha) k^2 (1 - \cos \theta_m)^2 \quad (36)$$

For a common absorption material with absorption coefficient $\alpha=90\%$, the reduction by the material will be 10 dB. At low frequencies this value is difficult to obtain, for high frequencies the possible reduction may be a bit more than 10 dB. However 10 dB is small compared to the amplification in the focus point, especially for spherical surfaces, see figure 12.

The effect of diffusion (or ‘scattering’ in the world of ray

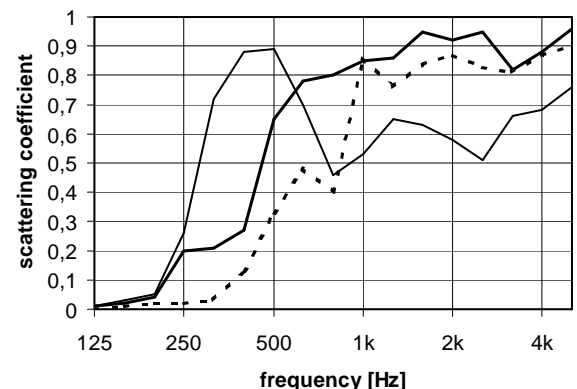


Figure 13. The scattering coefficient of three different diffusors. Solid line: modulated array, 6 periods, 8 wells/period, 0.17 m deep; dotted line: 6 semicylinders r=0.3 m; thin line: 3 semicylinders with 0.6 m flat sections [11]

tracing) might also be limited. Figure 13 shows the scattering coefficient of a few relatively good diffusors (from [11]).

The scattering coefficient is generally not more than 90%, indicating a 10 dB reduction of reflected energy. Especially at low frequencies this value is difficult to obtain.

For cylindrical shapes the required reduction is mostly significantly less as for spherical shapes (see fig.12). For cylinders absorption and/or diffusion might give sufficient reduction. For spherical shapes however the effect of both absorption and diffusion seems to be too limited to completely remove the focussing. An alternative would be to redirect the energy with surfaces of sufficient size so little energy will be reflected to the focal point. Fig. 14 shows the suppression of the specular energy with tilted panels, depending on the angle and panel size. For a reduction of 15 up to 20 dB a panel is needed of at least 2λ at 30° . For lower frequencies the reduction is less, but fortunately the amplification is also less.

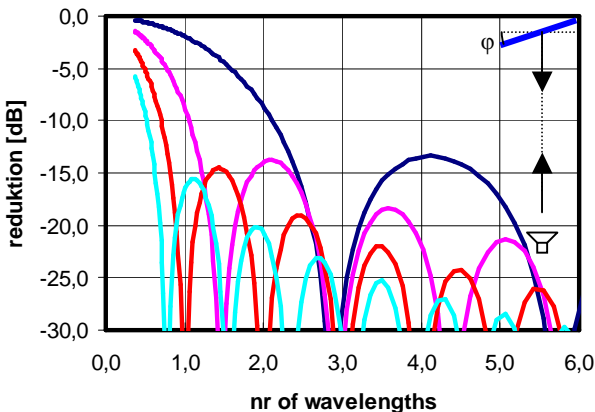


Figure 14. Reflected energy (back to the source) of a plane surface depending on the angle φ and the size of the panel. Horizontal axis: ratio of panel size to wavelengths, Vertical axis: reduction of the reflected sound relative to the panel at angle of 0 degrees. Source and receiver both in the far field. Blue: $\varphi = 10^\circ$; Violet: $\varphi = 20^\circ$; Red: $\varphi = 30^\circ$; Light blue: $\varphi = 40^\circ$; Calculated with (20)

5. TWO CASES

Tonhalle Düsseldorf

Before the renovation of 2005, the Tonhalle Düsseldorf had a shape close to a hemisphere. The section is shown in figure 15. The inner dome was made of wooden panels. The radius of the dome is about 18 m. The total visible reflecting concave surface is estimated to be 1/2 of an hemisphere. In this case the pressure in the focal point (re 1 m from the source) can be calculated from: $\Delta L = 10 \log k^2 - 20 \log(1/2)$. For 500

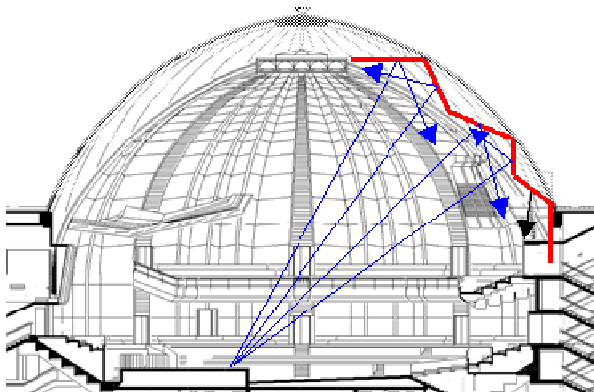


Figure 15. Section of the Tonhalle Düsseldorf: red: panels redirecting the reflections, either directly down towards audience or up in the dome.

Hz this results in a maximum amplification of 25 dB at a distance of 4 m from the source. Figure 2 shows an impulse response for a point symmetrically to the centre. The amplification found was around 20 dB. For other positions, more out of the focal point also amplifications are found, around 10 dB above the direct sound. The delay of the reflection is around 100 ms. The double beat was especially audible from percussion and piano. It was known as the “knocking ghost” (Klopfgeist).

Scale model research showed that diffusors would not completely take away the echo. The echo was completely removed with an acoustically transparent layer (wire mesh) at the position of the inner dome and redirecting panels between inner and outer dome, as described above (size 2λ at 250 Hz and placed at 30°) and as indicated in fig. 15 [3].

Ellipsoid meeting room

Fig.16 shows the cross section of an prolate ellipsoid meeting room in an office building. The floor cuts off part of the ellipsoid. The entrance is an opening at one of the ends. The walls are plastered. The curving of the room was made by hand, so there are some surface irregularities in the ellipsoid, estimated ± 1 cm.

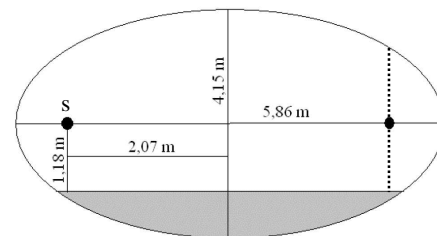


Figure 16. Dimensions of an ellipsoid meeting room, s=source, dotted line: calculation and measurement positions

With the source in one focal point, the SPL is measured along a vertical line through the other focal point. Fig. 17 shows a comparison with numerical calculations, based on (20). There is a good correspondence between measurement and numerical calculation. In the calculations the existence of the floor

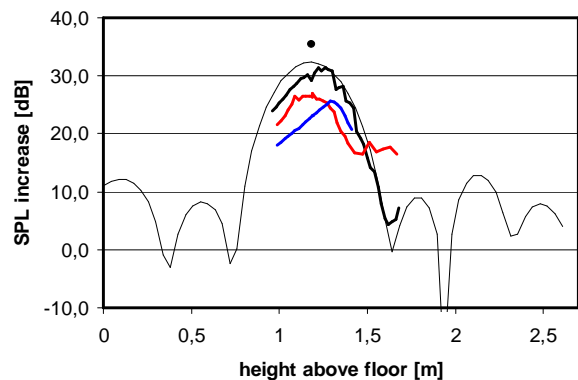


Figure 17. SPL increase (re direct sound) along a vertical line (fig.16), $f=630$ Hz (1/3 octave). Dot: calculated from (34); thin line: numerical calculation based on (20); solid line: measurement; blue line: measured with additional ceiling panel hung in the room; red line: wall absorption added to the room

and opening are accounted for. This is not the case for the result of (34) (the dot in fig. 17). By applying a ceiling panel and wall absorption it is possible to reduce the focussing by about 10 dB.

6. CONCLUSIONS

Within reasonable accuracy, the average sound pressure outside a focal point, from concave reflecting surfaces, can be estimated with geometrical methods. However these methods fail at the focal point. Based on wave extrapolation method, this paper has provided some mathematical formulations for the sound pressure in the focal point due to reflections from concave spherical surfaces. The approximations given can be used to calculate the sound field in and around the focal point. At the focal point the pressure depends on the wavelength at the opening angle of the sphere segment. It does not depend on the radius of the sphere. The width of the peak pressure is also related to the wavelength. For small wavelengths the amplification is high but the area small, while for lower frequencies the amplification is less, but the area is larger. The pressure at the focal point from a sphere is much higher than from a cylinder.

The validity of the basic integral describing the reflection from a curved surface (20) is verified with an experiment.

Generally the possible reduction of the focussing effect by absorbers or diffusers is insufficient to eliminate the focussing effect. For cylindrical shapes, which have much lower pressure in the focal line, these measures might be sufficient. In the case diffusers are not sufficient to reduce the focussing effect sufficiently, more drastic interventions are necessary such as changing the basic geometry or adding large reflectors or redirecting panels. Two cases are presented showing the high amplification in the focal point and ways to reduce it.

7. REFERENCES

- 1 A. Kircher, *Musurgia Universalis*, 1650
- 2 R.A.Metkemeijer, *The acoustics of the auditorium of the Royal Albert Hall before and after redevelopment*, Proceedings of the Institute of Acoustics, 2002
- 3 K.-H.Lorenz-K., M.Vercammen, *From 'Knocking ghost' to excellent acoustics – the new Tonhalle Düsseldorf: innovative design of a concert hall refurbishment*, Institute of Acoustics, 2006
- 4 M.L.S.Vercammen, *Sound Reflections from Concave Spherical Surfaces. Part I: Wave Field Approximation*, Acta Acustica 96 (2010)
- 5 M.L.S.Vercammen, *Sound Reflections from Concave Spherical Surfaces. PartII: Geometrical Acoustics and Engineering Approach*, Acta Acustica 96(2010)
- 6 J.H. Rindel, *Attenuation of Sound Reflections from Curved Surfaces*, Proceedings of 24th Conf. on Acoustics, Strbské Pleso, 194-197 (1985).
- 7 H.Kuttruff, *Room Acoustics*, Taylor & Francis, 1973, fourth edition 1999
- 8 H.Kuttruff, *Some remarks on the simulation of sound reflection from curved walls*. Acustica Vol. 77 (1993), p. 176
- 9 P.Jean, N. Noe, F. Gaudaire, *Calculation of tyre noise radiation with a mixed approach*, Acta Acustica, Vol. 00 (2007) 1-13
- 10 Y.Yamada, T.Hidaka, *Reflection of a spherical wave by acoustically hard, concave cylindrical walls based on the tangential plane approximation*, J.Acoust. Soc.Am.118(2), 2005
- 11 T.J.Cox, P.D'Antonio, *Acoustic Absorbers and Diffusers, Theory, Design and Application*, Spon Press, 2004